Computer Assisted Mechanics and Engineering Sciences, 12: 49–63, 2005.

Modeling and homogenization of foams

Tobias Ebinger, Holger Steeb, Stefan Diebels
Saarland University, Faculty of Material Science and Production Engineering
Chair of Applied Mechanics, 66123 Saarbrücken, Germany

(Received December 23, 2003)

The mechanical modeling of foams is discussed on a microscopic, mesoscopic and macroscopic scale. A homogenization procedure is proposed to relate the models and to give detailed insight into the deformation behavior of foams. The mesoscopic model of open-cell foams is based on beam elements and evaluated for regular hexagonal structures considering small deformations. This approach gives rise to a Cosserat continuum on the macroscopic scale. Especially the misfit in the parameters governing the standard macroscopic model can be explained by the proposed homogenization procedure. This misfit results from the neglect of the rotations of the cell walls, see Diebels and Steeb [6, 7].

1. Introduction and motivation

Foams have a large field of application due to their good suitability for insulation and cushoning, the possibility to absorb kinetic energy from impacts and the high stiffness in proportion to the density.

Normally it is very expensive to perform deformation tests experimentally, which are quite often required by norms and standards, see e.g. EuroNCAP (NCAP: New Car Assessment Program) for crash test used for ratings. Therefore, one aspires to simulate such tests numerically. Thus, the full set of material data is needed, which is quite challenging, especially for artificial materials with inherent microstructures.

Problems arise when a foam sample is tested in the laboratory: From continuum mechanics it is known that a purely elastic isotropic material is fully described by two independent material parameters, e.g. the engineering constants Young's modulus E and Poissons's ration ν, which can be determined by two independent experiments. But even for a foam, whose solid material is purely linear elastic, it can be shown, that the material is not fully described by two material parameters, because a third independent test would yield another set of material parameters even for small deformations. So often material parameters are stated with specification on which way they are obtained, while from theory they should be test-independent. These parameters can differ by a factor up to 1.5, see Gibson and Ashby [14] and Ebinger [8], who shows, that this effect may not be neglected.

In the present work, a microscopic model is proposed which gives insight into the deformation behavior of artificial open-cell foams. In the mesoscopic model the partition walls are represented by two-dimensional beam elements which allow for translational and rotational degrees of freedom and, as a consequence, allow for the transmission of forces and moments. Volumetrical averaging of the microscopic quantities like the forces and moments yields a set of macroscopic field quantities like stress and couple stress tensors. Therefore, the resulting continuum mechanical model should be able to transfer couple stresses, i.e. the model should be a Cosserat or micropolar continuum. Similar approaches for cellular material can be found e.g. by Lakes [20], Onck [22], Tekoglu and Onck [24] and Hohe and Becker [17].

It can be shown that the Cosserat theory is able to describe boundary layer effects, which can not be described by the classical Boltzmann continuum theory but which can be ovserved in the

laboratory. Figure 1 shows a shear test with the according boundary conditions and the resulting boundary layer effect for the couple stress tensor component $\langle \overline{M}_{32} \rangle$, where $\langle \bullet \rangle$ is related to an averaged macroscopic quantity.

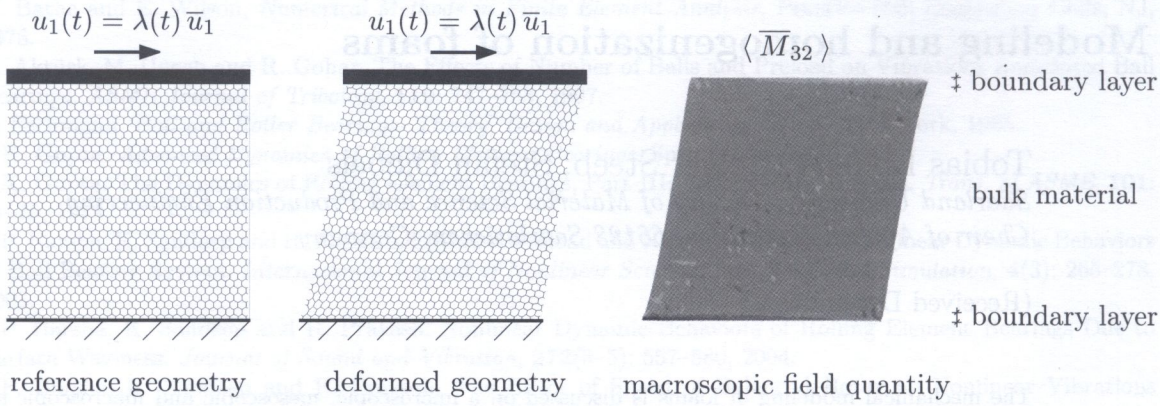

Fig. 1. Boundary layer effect for couple stress tensor $\langle \overline{M}_{32} \rangle$ in a shear test

A more detailed discussion of boundary layer effects can be found in Diebels and Steeb [6].

We want to remark, that such microscopically-driven results can also be found in the inner of a sample, c.f. Fig. 2. Thus, we investigate a pressure test with an imperfect microstructure. In the analyzed sample, the beam-like microstructure is assumed to be orthogonal. On the one hand, it can be observed that the macroscopic homogenized vertical stress component $\langle T_{22} \rangle$ is not influenced by the imperfections, while on the other hand couple stresses are observed as a result of the microscopic cell wall bending.

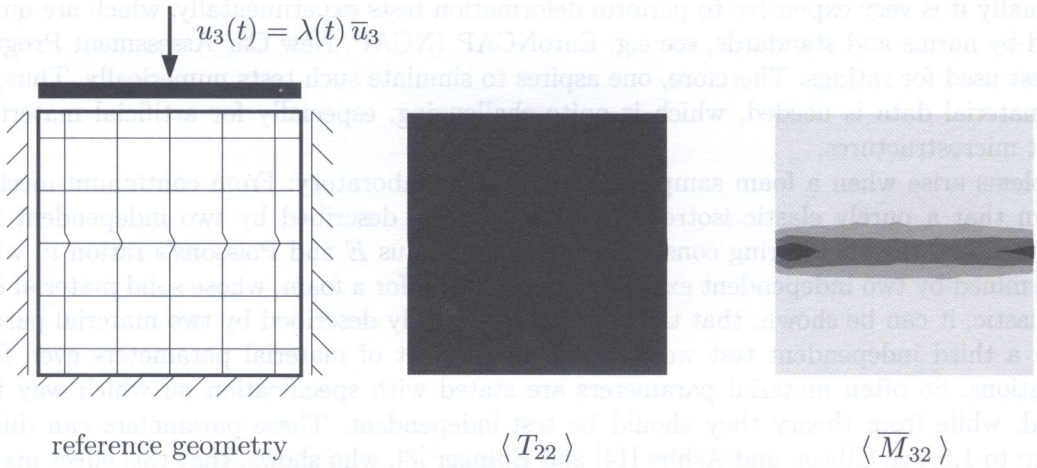

Fig. 2. Compression test with imperfect microstructure

The paper is organized as follows: First, a brief review of the microscopic model is given. Thereupon the idea of unit-cell models is given. In the following a homogenization procedure is presented which is based on volumetrical averages. The terms Testing Volume Element (TVE), see Huet [18], and Representative Volume Element (RVE), see e.g. Nemat–Nasser and Hori [21] and Kouznetsova [19], are introduced. Further requirements for them are stated, especially with respect to periodicity. The existence of forces and moments in the beam elements of the structure implies the existence of the stress and couple stress tensor on the macroscale. After that, a linear version of the macroscopic Cosserat theory is recalled and the weak form of the governing equations is presented. It follows an

investigation of the Hill condition, which yields a further criterion for determining the size of the TVE. The paper is closed with a discussion and outline.

2. Beam model

As discussed by Gibson and Ashby [14] or in several other applications, e.g. Onck, Andrews and Gibson [22], Schrad and Triantafyllidis [23], Becker and Hohe [17] and Diebels and Steeb [6], a microscopic model of open-cell foams can be built with beam structures. For simplicity a two-dimensional model is chosen, c.f. Fig. 3. The analyzed artificial foam geometry is a regular honeycomb structure[1].

Fig. 3. Regular honeycomb structure

Utilizing the periodicity of the geometry the beam structure can be replaced by a macroelement with equivalent stiffness, whereby rotations of the macroelement are allowed as can be seen in Fig. 4, where the smallest possible macroelement is shown. Continuity conditions for the macroelement have only to be fulfilled for the vertices but not for the whole boundary.

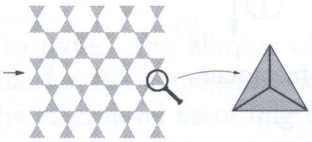

Fig. 4. Transition from honeycomb structure to macroelement

In principle, there is an arbitrary number of macroelements, but while the microscopic structure should be double symmetric to avoid effects introduced by asymmetric geometry, it follows that the macroelements should also be double symmetric. Thus, the beam structure can be replaced by macroelements without rotating them, see Fig. 5, which shows the smallest macroelement fulfilling that condition. This special macroelement is called unit-cell.

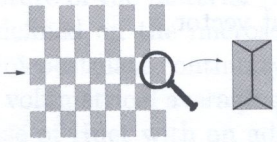

Fig. 5. Transition from honeycomb structure to unit-cell

Furthermore the unit-cell has the property that the moments at the vertices are zero for a unit-cell cut from the inner of a infinitely expanded honeycomb structure and loaded by shear, pressure or tension related to the results explained in Gibson and Asbhy [14]. This can also be shown for a finite structure applying appropriate boundary conditions.

[1] In our context "regular" means that all lengths and angles of the cell are identical.

The discrete stiffness matrix of the beam structure in a unit-cell can be derived starting from the stiffness matrices of the individual beams considering either the Bernoulli or Timoshenko[2] beam theory, e.g. the stiffness matrix of a single selective reduced integrated Timoshenko beam element is given by the algebraic system of equations

$$\underbrace{\frac{1}{l}\begin{bmatrix} EA & 0 & 0 & -EA & 0 & 0 \\ & GA_q & -c_1 GA_q & 0 & -GA_q & -c_1 GA_q \\ & & EI + c_2 GA_q & 0 & c_1 GA_q & -EI + c_2 GA_q \\ & & & EA & 0 & 0 \\ & & & & GA_q & c_1 GA_q \\ & & & & & EI + c_2 GA_q \end{bmatrix}}_{\mathsf{K}} \underbrace{\begin{bmatrix} u_1^{(i)} \\ u_3^{(i)} \\ \varphi^{(i)} \\ u_1^{(j)} \\ u_3^{(j)} \\ \varphi^{(j)} \end{bmatrix}}_{\mathbf{u}} = \underbrace{\begin{bmatrix} f_1^{(i)} \\ f_3^{(i)} \\ m^{(i)} \\ f_1^{(j)} \\ f_3^{(j)} \\ m^{(j)} \end{bmatrix}}_{\mathbf{f}}, \tag{1}$$

which is presented in matrix notation. In Eq. (1) A is the cross-sectional area, A_q the shear area, l the length of the beam, I the moment of inertia and E Young's modulus. c_1 and c_2 are constants with $c_1 = l/2$ and $c_2 = l^2/4$. The components of the generalized displacement vector $\mathbf{u}$ the displacements $u_a^{(b)}$ and the rotations $\varphi^{(b)}$ of the nodes, as well as the dual components of the generalized force vector $\mathbf{f}$, the discrete forces $f_a^{(b)}$ and discrete moments m^b acting on the beam ends, are visualized in Fig. 6.

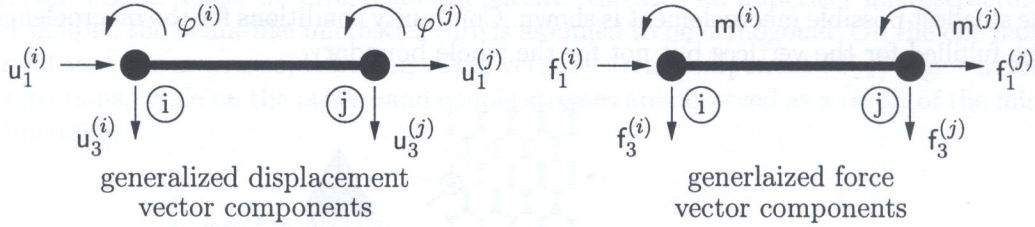

Fig. 6. Single Timoshenko beam element

After transforming the stiffness matrices from the local into the global coordinate system, assembling them into the global stiffness matrix and eliminating internal degrees of freedom (DOF) by static condensation, the stiffness matrix of the unit-cell is obtained, see Fig. 7. The algebraic system of equations for the unit-cell has the following format

$$\widehat{\mathsf{K}}\,\widehat{\mathbf{u}} = \widehat{\mathbf{f}}, \tag{2}$$

with the generalized displacement vector

$$\widehat{\mathbf{u}} = \left[\mathbf{u}^{(1)^{\mathrm{T}}}\,\mathbf{u}^{(2)^{\mathrm{T}}}\,\mathbf{u}^{(3)^{\mathrm{T}}}\,\mathbf{u}^{(4)^{\mathrm{T}}}\right]^{\mathrm{T}}, \tag{3}$$

and the generalized force vector

$$\widehat{\mathbf{f}} = \left[\mathbf{f}^{(1)^{\mathrm{T}}}\,\mathbf{f}^{(2)^{\mathrm{T}}}\,\mathbf{f}^{(3)^{\mathrm{T}}}\,\mathbf{f}^{(4)^{\mathrm{T}}}\right]^{\mathrm{T}}, \tag{4}$$

[2]In the present work we focus ourselves on Timoshenko beam elements on the microscale as the Timoshenko beam can be identified as a one-dimensional Cosserat formulation while the Euler–Bernoulli beam can be identified as a one-dimensional "restricted" Cosserat formulation. A "restricted" Cosserat theory is also called couple-stress theory.

using the abbreviations

$$\begin{aligned} \mathbf{u}^{(i)} &= \left[u_1^{(i)}\, u_3^{(i)}\, \varphi^{(i)}\right]^{\mathrm{T}}, \qquad i = 1, \ldots, 4, \\ \mathbf{f}^{(i)} &= \left[f_1^{(i)}\, f_3^{(i)}\, m^{(i)}\right]^{\mathrm{T}}, \qquad i = 1, \ldots, 4. \end{aligned} \tag{5}$$

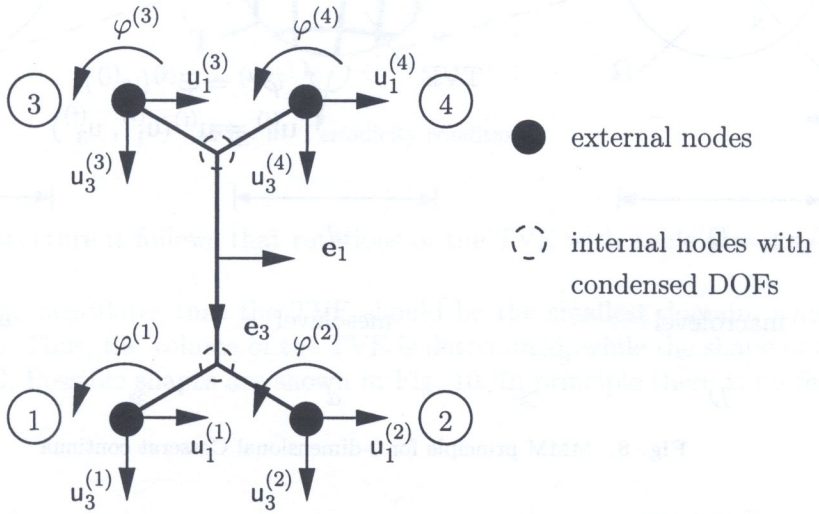

Fig. 7. Unit-cell with node numeration

The unit-cell, c.f. Fig. 7, can be used to reduce the number of degrees of freedom (DOF) in numerical simulations, but it is not suitable for the homogenization procedure, if one requires a homogenized quantity to be constant on the macrolevel according to a uniform deformation state, as will be shown in the next section.

3. Concept of homogenization theory

The goal of the homogenization theory is to calculate macroscopic averaged quantities from fluctuating fields on the microscale. The basic concept of the investigation is the so-called MMM principle visualized in Fig. 8 tracing back to Hashin [15].

Three different scales can be defined, namely the microscale δ, the mesoscale d and the macroscale D. The scales are separated, i.e. $\delta \ll d \ll D$. While the behavior on the macroscale is governed by a continuum mechanical model, the structure of the material (in the case under study: the pore structure and the individual cell walls) is defined on the microscale. A Testing Volume Element (TVE) is defined, see Huet [18]. Huet does not postulate continuity conditions for the TVE, but for the homogenization procedure performed by volumetrical averaging this condition is required. In the following we use the term "TVE" in the sense of Huet with an additional restriction of continuity. The average over a TVE smears out the fluctuations of the microscopic quantities, but it recovers the inhomogeneities being present on the macroscale. In contrast to the Representative Volume Element (RVE), see Nemat–Nasser and Hori [21], the TVE does not have to be representative in a statistical sense allowing for smaller volumes with changing geometry.

Following Kouznetsova [19], there are two definitions of the so-called RVE:

- *Strong formulation:* The first definition requires a RVE to be a statistically representative sample of the microstructure, i.e. to include virtually a sampling of all possible microstructural configurations that occur in the composite.

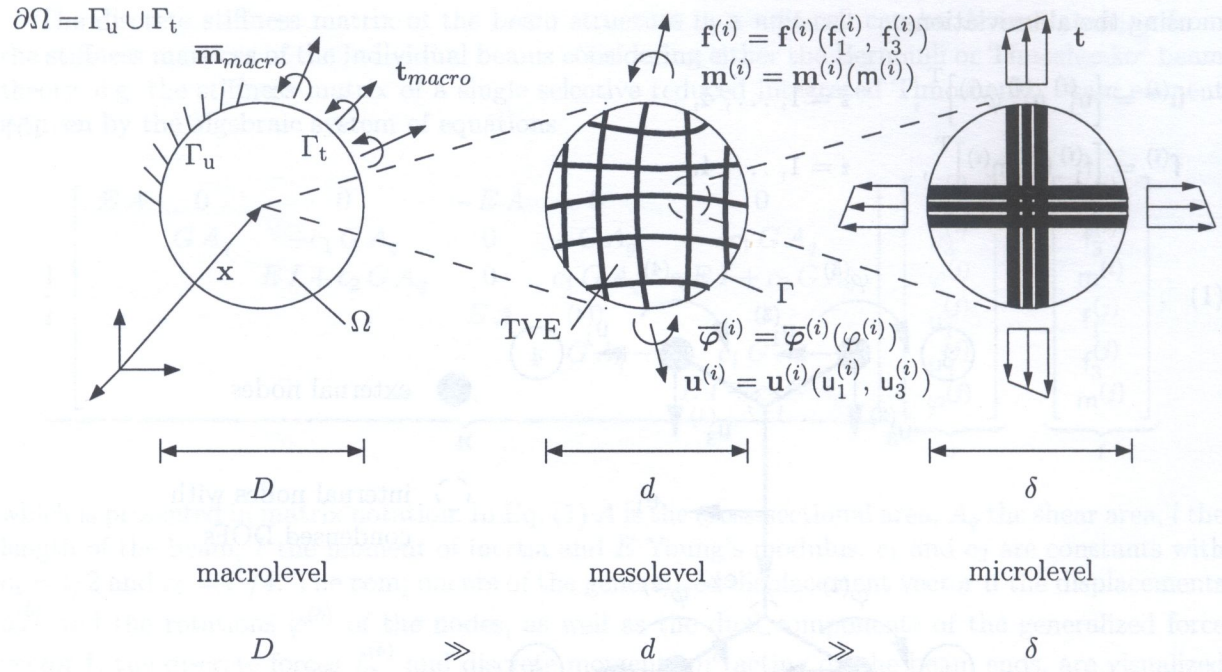

Fig. 8. MMM principle for 2-dimensional Cosserat continua

- *Weak formulation:* The second definition characterizes a RVE as the smallest microstructural volume that represents the overall macroscopic properties of interest with sufficient accuracy.

The first definition leads to considerably large RVEs in the case of non-regular and non-uniform microstructures. Very small RVEs can be obtained only for regular and uniform structures applying periodic boundary conditions in space.

The second definition leads to much smaller RVE sizes than the statistical definition described above. But in the present context (Diebels and Steeb [6]) the effective material properties derived by homogenization procedures may depend on the boundary conditions and deviations of geometry and material properties on the microscale. So, in the present work, the definition of the weak formulation of the RVE and the above given definition of the TVE are identical.

Furthermore, from a continuum mechanical point of view, the TVE plays the role of a material point, i.e. the smallest observable entity.

For the honeycomb structure under study it follows that the stiffness of the TVE is representative in a strong sense due to periodicity while the deformation of the TVE is only representative in a weak sense due to boundary conditions enabling the recovery of boundary layers and macroscopic inhomogeneities.

The selection of the domain Ω of the TVE is arbitrary at the moment. But now one postulates some requirements for the domain constraining the selection. The first postulate for the TVE is the mathematical definition of periodicity, see Cioranescu and Donato [2]

$$\int_{\Omega_0} (\Diamond)\, \mathrm{d}v = \int_{\Omega_1} (\Diamond)\, \mathrm{d}v, \tag{6}$$

where $(\Diamond)$ are arbitrary microscopic field quantities. The postulate should be fulfilled for uniform deformation states with boundary conditions representing an infinite expansion of the structure, so that one gets constant values for the homogenized quantities. The domain Ω_1 is obtained by translatoric transformation of the domain Ω_0, whereby $\mathbf{y}_0$ is the translation determining direction and amount of the displacement, see Fig. 9.

This postulate determines the volume fraction of the solid material to the void space in the inner of the domain and also feasible shapes of the boundary. From the special geometry of the considered

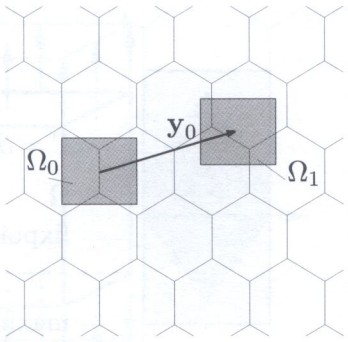

Fig. 9. Periodicity condition

regular hexagonal structure it follows that rotations of the TVE with angle $\varphi = \pm\pi/3$ should also yield feasible TVEs.

In a next step one postulates that the TVE should be the smallest domain, which fulfills the previous assumption. Thus, the volume of the TVE is determined, while the shape of the boundary is still undetermined. Possible shapes are shown in Fig. 10. In principle there is no reason to allow only convex shapes.

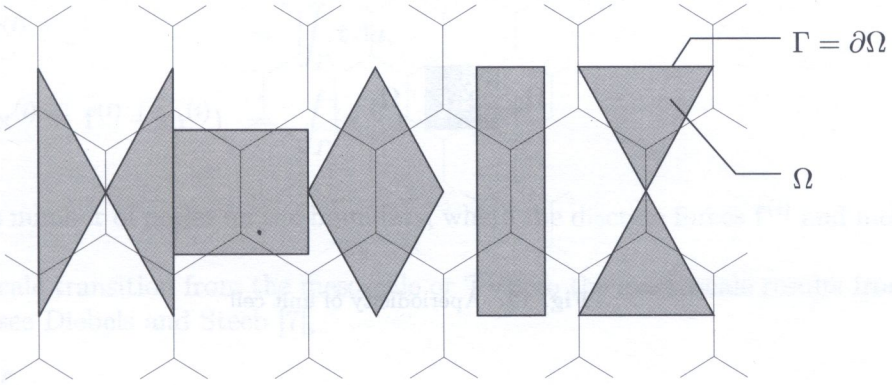

Fig. 10. Undefined boundary of the TVE

As one can show, all possible shapes can be constructed by polygons through fixpoints cutting a so-called maximum box, which can be constructed by the periodic length in each direction, see Fig. 11.

Now one has to demonstrate that the selection of the boundary Γ has no further influence on the homogenization process. For the stress and couple stress tensor this is obvious, while it is possible to choose the fixpoints as intersection points of the beam structure with the boundary, keeping in mind that a translation of the center of the TVE may not have any influence due to the periodicity condition.

After application of the homogenization procedure the strains and curvatures in the TVE are considered to be constant. Hence, the displacement field $\mathbf{u}(\mathbf{x})$ can only be distributed linearly. Now it can be shown, that for a bilinear distribution of a vector-valued variable, e.g. the displacement $\mathbf{u}$, which can be described by bilinear ansatz functions with discrete values at the fixpoints, where again the fixpoints are selected as the intersection points, the integral over the boundary $\int_\Gamma \mathbf{u} \otimes \mathbf{n}\, da$ is independent of the chosen feasible shape. $\mathbf{n}$ is the outward directed normal on the boundary Γ. It follows that the selection of the boundary has no influence on the calculation of the homogenized kinematical values of the TVE.

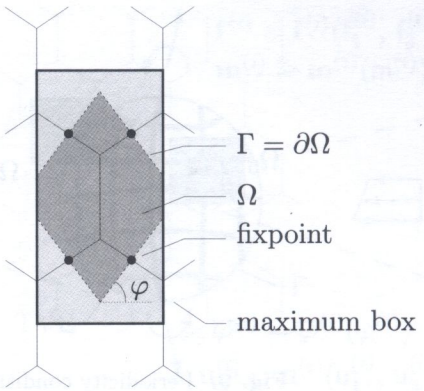

Fig. 11. Possible boundaries of the TVE

It can be shown that the mathematical definition of periodicity, c.f. Eq. (6), does not hold for this unit-cell, while e.g. a translation $\mathbf{y}_0$ with amount of the unit-cell width in horizontal direction would place the unit cell over void space with no stiffness, which is visualized in Fig. 12.

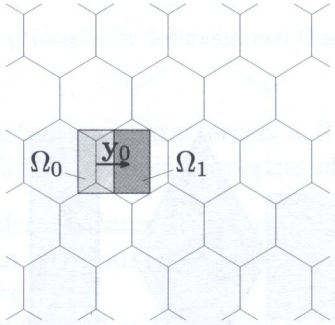

Fig. 12. Aperiodicity of unit cell

While the periodicity condition allows for arbitrary transformation vectors $\mathbf{y}_0$, see Fig. 9, the unit-cell fulfills the condition only for certain vectors $\mathbf{y}_0$, see Fig. 12. Thus, the unit-cell is not a TVE. But by adding the volumes Ω_0 and Ω_1 as shown in Fig. 12, i.e. blowing up the unit-cell in such a way, that it is space filling, the unit-cell becomes a TVE, c.f. Fig. 10. As can be seen, the stiffness matrix is not changed by blowing up the volume. Therefore the stiffness matrix of the unit-cell, equation (2), stated in the previous section can still be used for the TVE.

We want to remark, that the mentioned concepts according to homogenization are still general. According to the experimentally observed size effects in cellular materials higher order continua with inherent length parameter are taken into account on the macroscale. Thus, the classical homogenization concept which was originally developed for Boltzmann continua has to be extended, see Forest [12], Forest and Sab [13] and Kouznetsova [19].

The choice of a beam theory yields a first scale transition from the microscopic to the mesoscopic scale, i.e. the transformation from the stress distribution in the cross section to the equivalent forces and moments. Thus, a linear stress distribution over the height h of the cross section is assumed. Furthermore, according to scale separation, the general balances of continuum mechanics reduce to discrete equilibrium conditions on the mesoscale. If the field quantities under study are regular the volumetric contributions within the balance equations tend to zero with the order of $O(d^3/D^3)$ while the contribution of the flux terms tend to zero with $O(d^2/D^2)$, c.f. Fig. 13. Therein, d represents the characteristic size of the TVE and D is a characteristic dimension of the macroscopic problem as shown in Fig. 8.

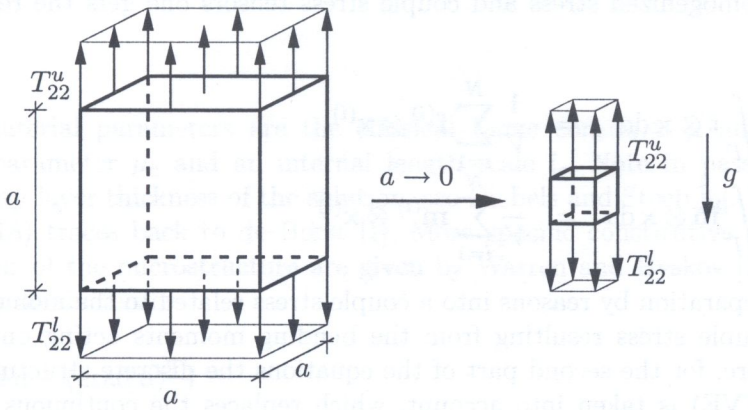

$$T_{22}^u\, a^2 = T_{22}^l\, a^2 + \rho\, g_2\, a^3 \qquad T_{22}^u\, a^2 \approx T_{22}^l\, a^2$$

Fig. 13. Neglection of volume forces due to scale separation

The corresponding equilibrium conditions for the forces $\mathbf{f}^{(i)}$ and moments $\mathbf{m}^{(i)}$ on the mesoscale are given by

$$\begin{aligned} \mathbf{0} &= \sum_{i=1}^{n} \mathbf{f}^{(i)} &&= \int_{\Gamma} \mathbf{t}\, da, \\ \mathbf{0} &= \sum_{i=1}^{n} (\mathbf{x}^{(i)} \times \mathbf{f}^{(i)} + \mathbf{m}^{(i)}) &&= \int_{\Gamma} (\mathbf{x} \times \mathbf{t} + \overline{\mathbf{m}}). \end{aligned} \tag{7}$$

Thereby n is the number of nodes on the boundary, where the discrete forces $\mathbf{f}^{(i)}$ and moments $\mathbf{m}^{(i)}$ are acting.

The second scale transition from the mesoscale or TVE to the macroscale results from volumetrical averaging, see Diebels and Steeb [7],

$$\langle\, \mathbf{A} \,\rangle := \frac{1}{V} \int_{\Omega} \mathbf{A}\, dv, \tag{8}$$

where $\mathbf{A}$ is a tensor of second order and V represents the volume of the TVE. For the following manipulations the identity

$$\mathbf{A}^{\mathrm{T}} = \operatorname{div}(\mathbf{x} \otimes \mathbf{A}) - \mathbf{x} \otimes \operatorname{div} \mathbf{A} \tag{9}$$

is needed. Considering the transposed of $\langle\, \mathbf{A} \,\rangle$, the generalized equilibrium condition $\operatorname{div} \mathbf{A} = \mathbf{0}$ and the divergence theorem, the averaged quantity reads

$$\langle\, \mathbf{A} \,\rangle^{\mathrm{T}} = \frac{1}{V} \int_{\Omega} \operatorname{div}(\mathbf{x} \otimes \mathbf{A})\, dv = \frac{1}{V} \int_{\Gamma} (\mathbf{x} \otimes \mathbf{A}) \cdot \mathbf{n}\, da. \tag{10}$$

If a Cauchy theorem is valid in the form $\mathbf{a} = \mathbf{A} \cdot \mathbf{n}$, the homogenized quantities can be computed from given boundary data in the form

$$\langle\, \mathbf{A} \,\rangle = \frac{1}{V} \int_{\Gamma} \mathbf{a} \otimes \mathbf{x}\, da, \tag{11}$$

where $\mathbf{x}$ is the so-called branch vector connecting the center of the TVE with the points along the boundary.

Thus, for the homogenized stress and couple stress tensors one gets the relations, see Diebels and Ehlers [5]

$$\begin{aligned} \langle \mathbf{T} \rangle &= \frac{1}{V} \int_{\Gamma} \mathbf{t} \otimes \mathbf{x} \, da &&= \frac{1}{V} \sum_{i=1}^{N} \mathbf{f}^{(i)} \otimes \mathbf{x}^{(i)}, \\ \langle \overline{\mathbf{M}} \rangle &= \frac{1}{V} \int_{\Gamma} \overline{\mathbf{m}} \otimes \mathbf{x} \, da &&= \frac{1}{V} \sum_{i=1}^{N} \mathbf{m}^{(i)} \otimes \mathbf{x}^{(i)}. \end{aligned} \tag{12}$$

In Eq. $(12)_2$ a separation by reasons into a couple stress related to the moment of the boundary tractions and a couple stress resulting from the bending moments acting on the boundary was applied. Furthermore, for the second part of the equations the discrete structure on the mesoscale (the scale of the TVE) is taken into account, which replaces the continuous distribution of the tractions $\mathbf{t}$ and couples $\overline{\mathbf{m}}$ by discrete forces $\mathbf{f}^{(i)}$ and moments $\mathbf{m}^{(i)}$.

Analogous considerations for granular assemblies can be found in Ehlers, Ramm, Diebels and d'Addetta [9].

4. Cosserat Theory

The Cosserat theory is an extended continuum mechanical description which takes care of independent rotational degrees of freedom, e.g. Cosserat and Cosserat [3], Eringen and Kafadar [11], Eringen [10] and Diebels [4]. In the present contribution only a geometrically linear version of the theory is presented which will be related to the results of the microscopic beam and material model.

Within the Cosserat approach a material point is regarded as a rigid body on the microscale. Therefore, the material point possesses 3 (2) translational and 3 (1) rotational degrees of freedom in the space (in the plane). The translational degrees of freedom are described by the displacements $\mathbf{u}$, the rotations are characterized in the geometrically linear setting by the angle of rotation $\overline{\boldsymbol{\varphi}}$. The linearized deformation measures of the Cosserat continum are the Cosserat strain tensor

$$\overline{\boldsymbol{\varepsilon}} = \operatorname{grad} \mathbf{u} + \overset{3}{\mathbf{E}} \cdot \overline{\boldsymbol{\varphi}} \tag{13}$$

and the curvature tensor

$$\overline{\boldsymbol{\kappa}} = \operatorname{grad} \overline{\boldsymbol{\varphi}}. \tag{14}$$

$\overset{3}{\mathbf{E}}$ represents the Ricci permutation tensor and "grad" is the gradient operator. A formal linearization of the general nonlinear kinematical quantities is discussed e.g. in Volk [26].

According to the extended kinematics, a Cosserat continuum is able to transfer stresses $\mathbf{T}$ and couple stresses $\overline{\mathbf{M}}$, which are energetically conjugated to the Cosserat strain $\overline{\boldsymbol{\varepsilon}}$ and the curvature $\overline{\boldsymbol{\kappa}}$ respectively. Thus, the equilibrium conditions are given for a body Ω without body forces and body couples by

$$\operatorname{div} \mathbf{T} = \mathbf{0} \tag{15}$$

representing the balance of linear moment and by

$$\mathbf{I} \times \mathbf{T} + \operatorname{div} \overline{\mathbf{M}} = \mathbf{0} \tag{16}$$

representing the balance of moment of momentum. In Eq. (16) the product $\mathbf{I} \times \mathbf{T}$ is twice the axial vector of the non-symmetric stress tensor.

The constitutive equations for linear elastic behavior are governed by the generalized Hooke's law in the form

$$\mathbf{T} = 2\,\mu \operatorname{sym} \overline{\boldsymbol{\varepsilon}} + 2\,\mu_c \operatorname{skw} \overline{\boldsymbol{\varepsilon}} + \lambda \, (\operatorname{tr} \overline{\boldsymbol{\varepsilon}}) \, \mathbf{I} \tag{17}$$

and

$$\overline{\mathbf{M}} = 2\,\mu_c\,(l_c)^2\,\overline{\boldsymbol{\kappa}}. \tag{18}$$

The involved material parameters are the classical Lamé constants μ and λ, an additional Cosserat stiffness parameter μ_c and an internal length scale l_c. Note in passing that l_c mainly governs the boundary layer thickness of the solution, see Diebels and Steeb [6]. The reduced ansatz according to Eq. (18) traces back to de Borst [1]. More specific constitutive equations based on symmetry conditions of the microstructure are given by Warren and Byskov [25]. The symmetric part of the Cosserat strain tensor

$$\operatorname{sym}\overline{\boldsymbol{\varepsilon}} = \frac{1}{2}\left(\operatorname{grad}\mathbf{u} + (\operatorname{grad}\mathbf{u})^{\mathrm{T}}\right) \tag{19}$$

is equivalent to the standard engineering strain measure while the skewsymmetric part

$$\operatorname{skw}\overline{\boldsymbol{\varepsilon}} = \frac{1}{2}\left(\operatorname{grad}\mathbf{u} - (\operatorname{grad}\mathbf{u})^{\mathrm{T}}\right) + \overset{3}{\mathbf{E}}\cdot\overline{\boldsymbol{\varphi}} \tag{20}$$

represents the difference between the continuum rotation and the independent rotation.

The set of governing partial differential equations can be solved numerically by the finite element method. Thus, the equations are transformed into a weak formulation by multiplying with test-functions $\delta\mathbf{u}$ and $\delta\overline{\boldsymbol{\varphi}}$ and integrating over the volume of the body Ω, see e.g. Diebels [4]. This yields

$$\begin{aligned} \int_\Omega \mathbf{T} : \operatorname{grad}\delta\mathbf{u}\,\mathrm{d}v &= \int_\Gamma \delta\mathbf{u}\cdot\mathbf{t}\,\mathrm{d}a, \\ \int_\Omega \left(-(\mathbf{I}\times\mathbf{T})\cdot\delta\overline{\boldsymbol{\varphi}} + \overline{\mathbf{M}} : \operatorname{grad}\delta\overline{\boldsymbol{\varphi}}\right)\mathrm{d}v &= \int_\Gamma \delta\overline{\boldsymbol{\varphi}}\cdot\overline{\mathbf{m}}\,\mathrm{d}a. \end{aligned} \tag{21}$$

The terms on the right hand of Eq. (12) are governed by the weak form of the Neumann boundary conditions for the tractions and the couples along the boundary.

5. Hill condition

The Hill condition [16] yields a further criterion, which should be fulfilled by the TVE. The Hill condition postulates the equivalence of the macroscopic and mesoscopic energy of the TVE. While only small deformations were considered for the Cosserat continuum, it is sufficient to use the linearized form of the Hill condition

$$W(\mathbf{x})_{\mathrm{lin}} = \overline{W}(\mathbf{x})_{\mathrm{lin}}, \tag{22}$$

where $\overline{W}(\mathbf{x})_{\mathrm{lin}}$ is the macroscopic homogenized linearized energy given by

$$\overline{W}(\mathbf{x})_{\mathrm{lin}} = \frac{1}{2}\langle\,\mathbf{T}\,\rangle : \langle\,\overline{\boldsymbol{\varepsilon}}\,\rangle + \frac{1}{2}\langle\,\overline{\mathbf{M}}\,\rangle : \langle\,\overline{\boldsymbol{\kappa}}\,\rangle \tag{23}$$

and $W(\mathbf{x})_{\mathrm{lin}}$ is the mesoscopic homogenized linearized energy given by

$$\begin{aligned} W(\mathbf{x})_{\mathrm{lin}} &= \frac{1}{2}\langle\,\mathbf{T} : \overline{\boldsymbol{\varepsilon}}\,\rangle + \frac{1}{2}\langle\,\overline{\mathbf{M}} : \overline{\boldsymbol{\kappa}}\,\rangle \\ &= \frac{1}{2V}\int_\Omega \mathbf{T} : \left(\operatorname{grad}\mathbf{u} + \overset{3}{\mathbf{E}}\cdot\overline{\boldsymbol{\varphi}}\right)\mathrm{d}v + \frac{1}{2V}\int_\Omega \overline{\mathbf{M}} : (\operatorname{grad}\overline{\boldsymbol{\varphi}})\,\mathrm{d}v. \end{aligned} \tag{24}$$

The linearized mesoscopic energy can be transformed using the identity

$$\operatorname{div}(\mathbf{T}\cdot\mathbf{u}) = (\operatorname{div}\mathbf{T}^{\mathrm{T}})\cdot\mathbf{u} + \mathbf{T}^{\mathrm{T}} : \operatorname{grad}\mathbf{u} \tag{25}$$

and the definition of the axial vector

$$\mathbf{I}\times\mathbf{T} = \overset{3}{\mathbf{E}} : \mathbf{T}^{\mathrm{T}} \tag{26}$$

into the form

$$W(\mathbf{x})_{\mathrm{lin}} = \frac{1}{2V}\int_{\Omega}\left[\operatorname{div}(\mathbf{T}^{\mathrm{T}}\cdot\mathbf{u}) + \operatorname{div}(\overline{\mathbf{M}}^{\mathrm{T}}\cdot\overline{\boldsymbol{\varphi}})\right]\,\mathrm{d}v. \tag{27}$$

Applying the divergence theorem, the volume integral can be transformed into a surface integral

$$W(\mathbf{x})_{\mathrm{lin}} = \frac{1}{2V}\int_{\Gamma}[\mathbf{t}\cdot\mathbf{u} + \overline{\mathbf{m}}\cdot\overline{\boldsymbol{\varphi}}]\,\mathrm{d}a. \tag{28}$$

Taking into account that the forces are acting only at discrete points of the surface of the TVE, the linearized mesoscopic average energy $W(\mathbf{x})_{\mathrm{lin}}$ for the Cosserat continuum reads

$$W(\mathbf{x})_{\mathrm{lin}} = \frac{1}{2V}\sum_{i=1}^{N}(\mathbf{f}^{(i)}\cdot\mathbf{u}^{(i)} + \mathbf{m}^{(i)}\cdot\overline{\boldsymbol{\varphi}}^{(i)}). \tag{29}$$

While the linearized mesoscopic energy is fully described by discrete values on the boundary of the TVE, one aspires to describe the linearized macroscopic average energy also by values on the boundary of the TVE.

The volume integral $\int_{\Omega}\overset{3}{\mathbf{E}}\cdot\overline{\boldsymbol{\varphi}}\,\mathrm{d}v$ can not easily be reformulated as a surface integral. Therefore a volumetric split is introduced for the bulk material (index: s) and the void space (index: v).

The energy is then given by the sum of the volumetrically weighted energies of the bulk material and the void space which is of course zero (regarding open-cell foams without pore pressure)

$$\begin{aligned}\overline{W}(\mathbf{x})_{\mathrm{lin}} &= \frac{V^s}{2V}\langle\,\mathbf{T}^s\,\rangle : \langle\,\overline{\boldsymbol{\varepsilon}}^s\,\rangle + \frac{V^s}{2V}\langle\,\overline{\mathbf{M}}^s\,\rangle : \langle\,\overline{\boldsymbol{\kappa}}^s\,\rangle + \frac{V^v}{2V}\langle\,\mathbf{T}^v\,\rangle : \langle\,\overline{\boldsymbol{\varepsilon}}^v\,\rangle + \frac{V^v}{2V}\langle\,\overline{\mathbf{M}}^v\,\rangle : \langle\,\overline{\boldsymbol{\kappa}}^v\,\rangle \\ &= \frac{V^s}{2V}\langle\,\mathbf{T}^s\,\rangle : \langle\,\overline{\boldsymbol{\varepsilon}}^s\,\rangle + \frac{V^s}{2V}\langle\,\overline{\mathbf{M}}^s\,\rangle : \langle\,\overline{\boldsymbol{\kappa}}^s\,\rangle.\end{aligned} \tag{30}$$

The definitions of the average stress tensor and average couple stress tensor for the bulk material read

$$\begin{aligned}\langle\,\mathbf{T}^s\,\rangle &= \frac{1}{V^s}\sum_{i=1}^{N}\mathbf{f}^{(i)}\otimes\mathbf{x}^{(i)}, \\ \langle\,\overline{\mathbf{M}}^s\,\rangle &= \frac{1}{V^s}\sum_{i=1}^{N}\mathbf{m}^{(i)}\otimes\mathbf{x}^{(i)}.\end{aligned} \tag{31}$$

Analogously, the averaged linearized Cosserat strain tensor and the curvature tensor for the bulk material read

$$\begin{aligned}\langle\,\overline{\boldsymbol{\varepsilon}}^s\,\rangle &= \frac{1}{V^s}\int_{\Gamma^s}\mathbf{u}\otimes\mathbf{n}\,\mathrm{d}a + \frac{1}{V^s}\int_{\Omega^s}\overset{3}{\mathbf{E}}\cdot\overline{\boldsymbol{\varphi}}\,\mathrm{d}v, \\ \langle\,\overline{\boldsymbol{\kappa}}^s\,\rangle &= \frac{1}{V^s}\int_{\Gamma^s}\overline{\boldsymbol{\varphi}}\otimes\mathbf{n}\,\mathrm{d}a.\end{aligned} \tag{32}$$

In the following only structures modeled by Timoshenko beam elements on the mesoscale are considered. According to the beam theory the rotations in the cross section perpendicular to the beam axis are constant, which is known as the second Euler–Bernoulli hypothesis. Thus, as standard in beam theories, the volume integral $\int_{\Omega^s}(\bullet)\,\mathrm{d}v$ can be reduced to a line integral $\int_{\Lambda^s}(\bullet)\,\mathrm{d}l$ over the beam length of each beam

$$\frac{1}{V^s}\int_{\Omega^s}\overset{3}{\mathbf{E}}\cdot\overline{\varphi}\,\mathrm{d}v=\frac{1}{L^s}\int_{\Lambda^s}\overset{3}{\mathbf{E}}\cdot\overline{\varphi}\,\mathrm{d}l. \tag{33}$$

In a next step, one can show, which standardized deformation states yield non-zero values for the integral (only for modes with bending).

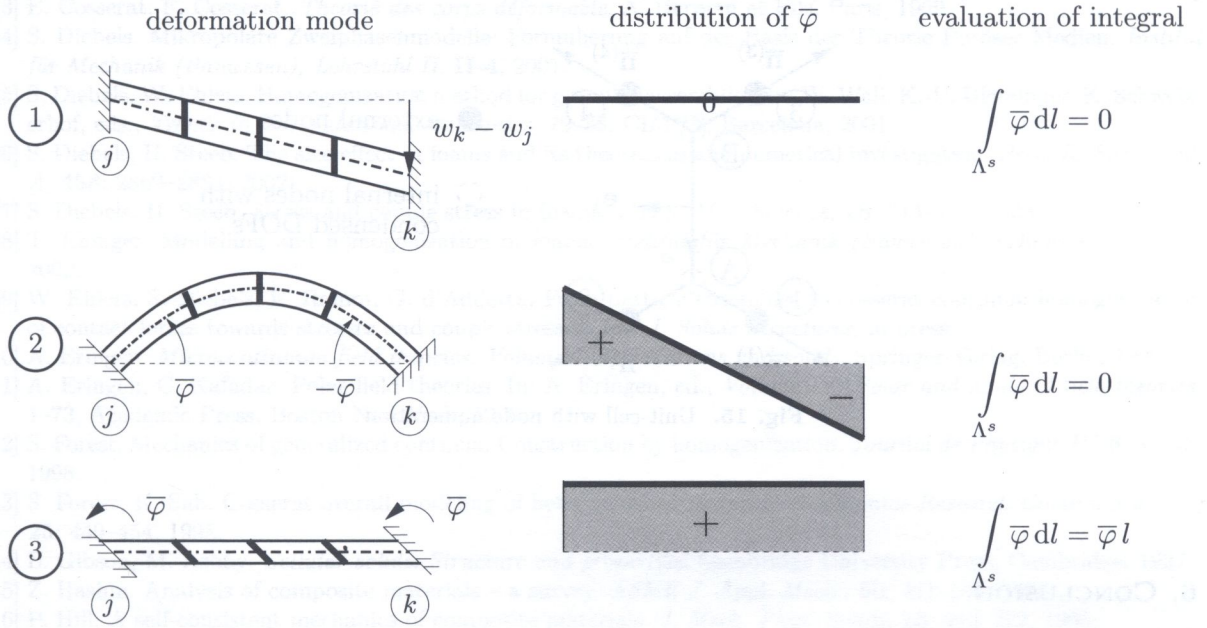

Fig. 14. Deformation modes

As can be seen, only one deformation mode has influence on that integral enabling the interpretation of this additional part on the macroscopic linearized Cosserat strain tensor as internal shear.

For the regular hexagonal structure, c.f. Fig. 15, it follows by evaluating the integral for the special geometry

$$\begin{aligned}\frac{1}{L^s}\int_{\Lambda^s}\overset{3}{\mathbf{E}}\cdot\overline{\varphi}\,\mathrm{d}l &= \frac{1}{3\,l}\overset{3}{\mathbf{E}}\cdot\left[\sum_{i=1}^{5}(w_j^{(i)}-w_k^{(i)})\right]\\ &= \frac{1}{3\,l}\overset{3}{\mathbf{E}}\cdot\left[\frac{1}{2}(u_1^{(1)}+u_1^{(2)}-u_1^{(3)}-u_1^{(4)})+\frac{\sqrt{3}}{2}(u_3^{(1)}-u_3^{(2)}+u_3^{(3)}-u_3^{(4)})\right]\mathbf{e}_2,\end{aligned} \tag{34}$$

with the displacement vector components $u_a^{(i)}$ as shown in Fig. 7. While for Eq. (34) a distinction between displacements in the local and global coordinate system is necessary, for the displacements in the local coordinate system the notation $w_a^{(i)}$ is used as visualized in Fig. 14. It can be seen that Eq. (34) is independent of the displacements of the internal nodes A and B.

While the displacements and rotations are constant in the cross section, the displacements and rotations at the top and bottom of the beam provide no contribution to the integral. Hence, only the

integral for the cross section on the free beam ends has to be evaluated, if they are cut perpendicular to the beam axis

$$\begin{aligned} \frac{1}{V_s}\int_{\Gamma_s} \mathbf{u}\otimes\mathbf{n}\,da &= \frac{b\,h}{V_s}\sum_{i=1}^{4}(\mathbf{u}^{(i)}\otimes\overline{\mathbf{n}}^{(i)}), \\ \frac{1}{V_s}\int_{\Gamma_s} \overline{\boldsymbol{\varphi}}\otimes\mathbf{n}\,da &= \frac{b\,h}{V_s}\sum_{i=1}^{4}(\overline{\boldsymbol{\varphi}}^{(i)}\otimes\overline{\mathbf{n}}^{(i)}), \end{aligned} \tag{35}$$

where $\overline{\mathbf{n}}^{(i)}$ are the outward directed normal vectors of the beam axis, c.f. Fig. 15, which are independent of the shape of the boundary.

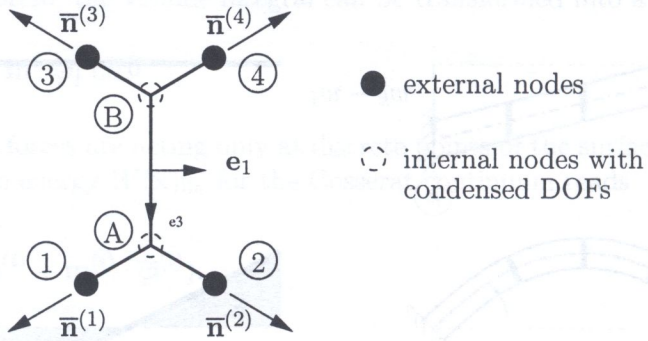

Fig. 15. Unit-cell with node numeration

6. Conclusion

In the present work, we have developed a multiscale approach for cellular materials, including homogenization concepts for micropolar elasticity on the macroscale. Thus, the experimentally observed size effects can be captured.

The energy due to curvatures in connection with couple stresses expose a boundary layer effect similar to that one of the couple stress tensor component $\langle\, \overline{M}_{32} \,\rangle$, which is visualized in Fig. 16.

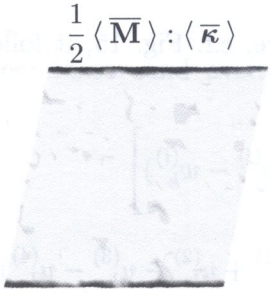

Fig. 16. Energy due to curvatures in shear test

Ebinger [8] has shown for the shear test, represented in Fig. 1, that taking into account rotational effects on the meso- and macroscopic level reduces the difference between mesoscopic energy given by $W(\mathbf{x})_{\text{lin}}$ and macroscopic energy given by $\overline{W}(\mathbf{x})_{\text{lin}}$ from about 7% to 1.5% of the mesoscopic energy. Therefore rotational effects have to be taken into account. While in the inner of a structure they contribute barely to the energy, at the boundary where boundary layer effects appear they

may not be neglected. Neglection explains the misfit of material parameters within the framework of the standard continuum mechanical setting.

By volumetrical split of the structure into bulk material and void space, an interpretation of the term $\int_\Omega \overset{3}{\mathbf{E}} \cdot \overline{\varphi}\, dv$, which appears in the homogenized linearized Cosserat strain tensor, can be given.

References

[1] R. de Borst. Numerical modelling of bifurcation and localization in cohesive-frictional materials. *Pageoph.*, **137**: 386–390, 1991.

[2] D. Cioranescu, P. Donato. *An introduction to homogenization.* Oxford University Press, Oxford, 1999.

[3] E. Cosserat, F. Cosserat. *Theorié des corps déformable.* A. Herman et Fils, Paris, 1909.

[4] S. Diebels. Mikropolare Zweiphasenmodelle: Formulierung auf der Basis der Theorie Poröser Medien. *Institut für Mechanik (Bauwesen), Lehrstuhl II,* **II-4**, 2001.

[5] S. Diebels, W. Ehlers. Homogenization method for granular assemblies. In: W. Wall, K.-U. Bletzinger, K. Schweizerhof, eds., *Trends in Computational Mechanics,* 79–88. CIMNE, Barcelona, 2001.

[6] S. Diebels, H. Steeb. The size effect in foams and its theoretical and numerical investigation. *Proc. R. Soc. Lond. A,* **458**: 2869–2883, 2002.

[7] S. Diebels, H. Steeb. Stress and couple stress in foams. *Comp. Mat. Science,* **28**: 714–722, 2003.

[8] T. Ebinger. Modelling and homogenization of foams. *Institut für Mechanik (Bauwesen), Lehrstuhl II,* **II-23**, 2002.

[9] W. Ehlers, S. Diebels, E. Ramm, G. d'Addetta. From particle ensembles to cosserat continua: homogenization of contact forces towards stresses and couple stresses. *Int. J. Solids Structures,* in press.

[10] A. Eringen. *Microcontinuum field theories. Volume I: Foundations and solids.* Springer-Verlag, Berlin, 1999.

[11] A. Eringen, C. Kafadar. Polar field theories. In: A. Eringen, ed., *Volume IV: Polar and nonlocal field theories,* 1–73, Academic Press, Boston-New York, 1976.

[12] S. Forest. Mechanics of generalized continua: Construction by homogenization. *Journal de Physique IV,* **8**: 39–48, 1998.

[13] S. Forest, K. Sab. Cosserat overall modeling of heterogeneous materials. *Mechanics Research Communications,* **25**: 449–454, 1998.

[14] L. Gibson, M. Ashby. *Cellular solids. Structure and properties.* Cambridge University Press, Cambridge, 1997.

[15] Z. Hashin. Analysis of composite materials – a survey. *ASME J. Appl. Mech.,* **50**: 481–505, 1983.

[16] P. Hill. A self-consistent mechanics of composite materials. *J. Mech. Phys. Solids,* **13**: 213–222, 1965.

[17] J. Hohe, W. Becker. Effective stress-strain relations for two-dimensional cores: Homogenization, material models and properties. *Appl. Mech. Rev.,* **55**: 61–87, 2002.

[18] C. Huet. An integrated micromechanics and statistical continuum thermodynamics approach for studying the fracture behaviour of microcracked heterogeneous materials with delayed response. *Eng. Fracture Mech.,* **58**: 459–556, 1997.

[19] V. Kouznetsova. *Computational homogenization for the multi-scale analysis of multi-phase materials.* Technical University Eindhoven, Eindhoven, 2002.

[20] R. Lakes. Experimental microelasticity of two porous solids. *Int. J. Solids Structures,* **22**: 55–63, 1986.

[21] S. Nemat-Nasser, M. Hori. *Micromechanics: Overall properties of heterogeneous materials.* Elsevier, Amsterdam, 1993.

[22] P. Onck, E. Andrews, L. Gibson. Size effects in ductile cellular solids. Part I: Modeling. *Int. J. Mech. Sci.,* **43**: 681–699, 2001.

[23] M. Schrad, N. Triantafyllidis. Scale effects in media with periodic and nearly periodic microstructures, Part I: Macroscopic properties. *ASME J. Appl. Mech.,* **64**: 751–762, 1997.

[24] C. Tekoglu and P. R. Onck. A comparison of discrete and Cosserat continuum analyses for cellular materials. In: J. Banhart, N. Fleck, eds., *Cellular Metals and Metal Forming Technology,* MIT-Verlag, 2003, to appear.

[25] W. Warren, E. Byskov. Three-field symmetry restrictions on two-dimenional micropolar materials. *Eur. J. Mech., A/Solids,* **21**: 779–792, 2002.

[26] W. Volk. Untersuchung des Lokalisierungsverhaltens mikropolarer poröser Medien. *Institut für Mechanik (Bauwesen), Lehrstuhl II,* **II-2**, 1999.